4th International Conference on Mechanical Engineering, December26-28, 2001, Dhaka, Bangladesh/pp.97-105

Keynote Paper

INTERACTION OF THERMOACOUSTIC WAVES AND BUOYANCY-INDUCED FLOWS IN AN ENCLOSURE

Bakhtier Farouk and Murat K. Aktas
Department of Mechanical Engineering and Mechanics, Drexel University
3141 Chestnut Street, Philadelphia, PA 19104 USA

Abstract The behavior of thermoacoustic waves in a nitrogen-filled two-dimensional cavity is numerically studied. The vertical walls of the cavity are heated or cooled to generate the thermoacoustic waves. Both impulsive and gradual change of the wall temperatures was considered. When a vertical wall is impulsively and nonuniformly heated, the resulting waves induce remarkable two-dimensional flows within the enclosure. The observed thermoacoustic waves oscillate and eventually decay due to the viscosity and thermal conductivity of the fluid. Effects of thermoacoustic wave motion on the developing natural convection process in a compressible gas-filled square enclosure were investigated. In the cases considered, the left wall temperature is raised impulsively or gradually while the right wall is held at a specified temperature. The top and the bottom walls of the enclosure considered are thermally insulated. The numerical solutions were obtained by employing a highly accurate flux corrected transport (FCT) algorithm for the convection terms and by coupling these to the viscous and diffusive terms of the full Navier-Stokes equations. The strength of the pressure waves associated with the thermoacoustic effect and resulting flow patterns are found to be strongly correlated to the rapidity of the wall heating process. Fluid thermal diffusivity was found to affect the strength of the thermoacoustic waves and the resulting interaction with the buoyancy-induced flow.

Keywords: Thermoacoustic waves, buoyancy-induced convection, flux-corrected transport algorithm.

INTRODUCTION

When a compressible fluid is subjected to a rapid temperature increase at a solid wall, part of the fluid in the immediate vicinity of the boundary expands. This gives rise to a fast increase in the local pressure, and leads to the production of pressure waves called thermoacoustic waves. The heat transfer effects of such waves may be very significant when the fluid is close to the thermodynamic critical point or when other modes of convection are weak or absent. This motion may cause unwanted disturbances in otherwise static processes like cryogenic storage or may introduce a convective heat transfer mode to the systems in zero-gravity environment where it is assumed that conduction is the only heat transfer mode.

The problem of thermoacoustic waves in a quiescent semi-infinite body of a perfect gas, subjected to a step change in temperature at the solid wall was studied analytically (Trilling, 1955) in order to determine how the sound intensity depends on the wall temperature history. The one-dimensional compressible flow equations were linearized and a closed-form asymptotic solution was obtained using a Laplace transform technique. A simplified model (the hyperbolic equation of conduction) for thermoacoustic motion was compared with one-dimensional Navier-Stokes equations model of the phenomena and limitations of the simplified approach was discussed (Churchill and Brown, 1987). A more general class of solutions for the thermoacoustic waves was obtained by using the Laplace transform method with numerical inversion for equations of the linear wave model for step and gradual changes in the boundary temperature (Huang and Bau, 1995). The equations of the nonlinear wave model were numerically solved using finite differences scheme modified with a Galerkin finite element interpolation in space. A similar analysis for thermoacoustic waves in a confined medium was repeated more recently (Huang and Bau, 1997). In both geometries the medium considered was a gas with Prandtl number of 0.75. Thermoacoustic convection phenomena were experimentally investigated in a cylinder containing air with temperature measurements in normal and reduced gravity environment (Parang and Salah-Eddine, 1984). No pressure measurement was reported. Experimental measurements of pressure waves generated by rapid heating of a surface were reported in a relatively recent paper (Brown and Churchill, 1995).

Numerical studies of one and two dimensional thermoacoustic waves in a confined region have been carried out (Ozoe et al., 1980; Ozoe et al., 1990). These computational studies describe finite-difference calculations of the compressible Navier-Stokes equations for a gas with temperature-independent thermophysical properties. The solutions were obtained by employing first-order upwind schemes to solve the governing equations, and as a consequence, the results showed effects of substantial numerical diffusion. Also, no special attention was paid for preserving the accuracy of the reflected acoustic waves from rigid walls. The mechanisms of heat and mass transport in a side-heated square cavity filled with a near-critical fluid were explored in (Zappoli et al., 1996), with special emphasis on the interplay between buoyancy-driven convection and the piston effect. In a recent paper, it was shown that rapid heating of a solid surface bounding a region of gas generates a slightly supersonic wave with positive amplitude in pressure, temperature, density and mass velocity (Brown and Churchill, 1999). The one-dimensional predictions were in good qualitative agreement with prior experimental measurements of the shape, amplitude and rate of decay of the pressure waves. Using a high order numerical scheme, the early time behavior of thermoacoustic waves in a compressible-fluid filled cavity was predicted with a computational study (Farouk et al., 2000) in which temperature dependent fluid properties were used.

In the present paper, the effects of thermoacoustic waves on buoyancy-induced flow fields are studied for an enclosure (Fig. 1). The horizontal walls of the square enclosure are considered to be insulated whereas the vertical walls are isothermal. Initially the gas and all walls are in thermal equilibrium ($T = T_R$ everywhere). At t>0, the left wall temperature is increased to a value T_L ($T_L > T_R$) either suddenly or gradually. The strength of the thermoacoustic waves depend on the rapidity of the wall heating, and the interaction effects are significant only for the early times. We also investigate the effects of fluid properties on the interaction process.

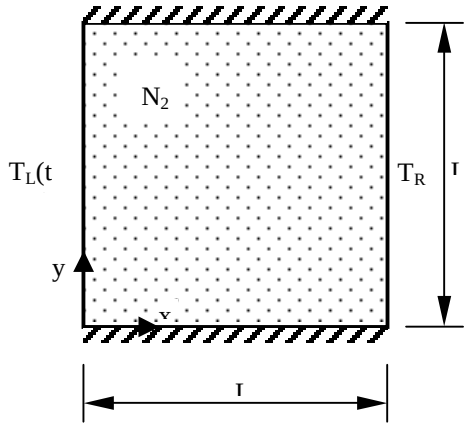

Fig.1 Geometry and the boundary conditions of the problem.

MATHEMATICAL MODEL

Interaction of thermoacoustic waves and buoyancy problem is described by the Navier-Stokes equations for a compressible fluid. These equations is expressed in vector form as

$$\frac{\partial \mathbf{U}}{\partial t}+\frac{\partial \mathbf{F}}{\partial x}+\frac{\partial \mathbf{G}}{\partial y}=\frac{\partial \mathbf{F_v}}{\partial x}+\frac{\partial \mathbf{G_v}}{\partial y}+\mathbf{B} \qquad (1)$$

where t is time and x and y refers to the Cartesian coordinates. The vectors represent:

$$\mathbf{U}=\begin{bmatrix}\rho\\ \rho u\\ \rho v\\ E\end{bmatrix} \qquad (2a)$$

$$\mathbf{F}=\begin{bmatrix}\rho u\\ \rho u^2+p\\ \rho uv\\ (E+p)u\end{bmatrix} \qquad \mathbf{G}=\begin{bmatrix}\rho v\\ \rho uv\\ \rho v^2+p\\ (E+p)v\end{bmatrix} \qquad (2b, c)$$

$$\mathbf{F_v}=\begin{bmatrix}0\\ \tau_{xx}\\ \tau_{xy}\\ q_x\end{bmatrix} \qquad \mathbf{G_v}=\begin{bmatrix}0\\ \tau_{xy}\\ \tau_{yy}\\ q_y\end{bmatrix} \qquad (2d, e)$$

$$\mathbf{B}=\begin{bmatrix}0\\ 0\\ \rho g\\ 0\end{bmatrix} \qquad (2f)$$

Where ρ is density, u and v are velocity components, g is gravitational acceleration, E is the total energy.

$$E=e+\frac{1}{2}\rho(u^2+v^2) \qquad (3)$$

Here e is the internal energy and p is pressure. The components of the stress tensor τ are:

$$\tau_{xx}=2\mu\frac{\partial u}{\partial x}-\frac{2}{3}\mu\nabla.\mathbf{v} \qquad (4a)$$

$$\tau_{yy}=2\mu\frac{\partial v}{\partial y}-\frac{2}{3}\mu\nabla.\mathbf{v} \qquad (4b)$$

$$\tau_{xy} = \mu\left(\frac{\partial u}{\partial y} + \frac{\partial v}{\partial x}\right) \qquad (4c)$$

Where μ is the dynamic viscosity and $\nabla.\mathbf{v}$ is the divergence of the velocity vector. The components of the heat-flux vector are written as

$$q_x = -k\frac{\partial T}{\partial x} \qquad q_y = -k\frac{\partial T}{\partial y} \qquad (5a, b)$$

where k is thermal conductivity and T is temperature. The viscous dissipation terms have been omitted from the energy equation since they are negligibly small in low Mach number flows. The temperature is related to the density and pressure through the ideal-gas law:

$$p = \rho RT \qquad (6)$$

Where R is the specific gas constant of the medium.

NUMERICAL SCHEME

The governing equations (except for the diffusion terms) are discretized using a control-volume-based finite-volume method based on the flux-corrected transport (FCT) algorithm. FCT is a high order, nonlinear monotone scheme designed to solve a general one-dimensional continuity equation with appropriate source terms. Time-step splitting technique is used to solve the two-dimensional problem addressed here. Further details of the FCT algorithm used here are documented in (Boris et al., 1993). The diffusion terms (the viscous term in the momentum equations and the conduction terms in the energy equation) were discretized using the central-difference approach and the time-splitting technique was used to include the terms in the numerical scheme. Time-splitting technique was also used to include the gravity term in the y-momentum equation.

No-slip boundary conditions were used for all the solid walls. Time-dependent boundary conditions for the vertical walls and zero-gradient temperature boundary conditions for the horizontal walls were used. A high-order non-dissipative algorithm such as FCT requires rigorous formulation of the boundary conditions. Otherwise, numerical solutions may show spurious wave reflections at the regions close to boundaries and nonphysical oscillations arising from instabilities. In the present computational method, the treatment proposed by (Poinsot and Lele, 1992) was followed for implementing the boundary conditions for the density. Along any solid wall, the density is calculated from

$$\left(\frac{\partial \rho}{\partial t}\right)_M + \frac{1}{c_M}\left(\frac{\partial p}{\partial n} + \rho c\frac{\partial u_n}{\partial n}\right)_M = 0 \qquad (7)$$

where c_M is the acoustic speed, M indicates the location of the wall and n is the direction normal to the wall.

RESULTS AND DISCUSSION

Numerical simulations of the thermoacoustic wave motion and its interactions with the buoyancy-induced flow fields were performed for a square enclosure filled with nitrogen gas, initially quiescent at 1 atm pressure and 300 K temperature. For all computations, non-uniform grid structure was employed with 141×141 computational cells. Variation of the fluid properties with temperature was taken into account. Results of our prior investigation (Farouk et al., 1991) on the very short time behavior of the thermoacoustic waves generated by impulsive and gradual heating of a wall were in very good agreement with the results given in the literature. In the present study, longer time behavior of the pressure waves produced by a step change (impulsive heating) at the left wall temperature of the enclosure was investigated. For impulsive heating, the left wall temperature is given by

$$T_L = \begin{cases} T_0 & ; t = 0 \\ T_0(A+1) & ; t > 0 \end{cases} \qquad (8)$$

where T_0 is the initial temperature ($T_0 = T_R$) and A is the overheat ratio.

$$A = \frac{T_L - T_R}{T_R} \qquad (9)$$

Short time solutions

Figure 2 shows the resulting pressure wave for sudden heating (A = 1.0) along the horizontal mid-plane. The nondimensional pressure p^* profiles are shown at selected times $\hat{t}$ = 0.25, 1.0, 1.5 and 2.0. The arrows in the figure indicate the direction of the wave motion. The overheat ratio for the results shown in Fig. 2 is 1.0. For the short amount of time that the thermoacoustic wave propagation displayed in this figure, the effects of horizontal walls on the wave propagating along the horizontal mid-plane were negligible.

A sharp front and a long tail characterize the pressure wave. With increasing time, the width of the peak broadens and the height decreases. When the pressure wave encounters the solid wall on the right side, it is reflected and its amplitude increases. Due to the relatively high value of A, the wave actually travels faster than the reference acoustic speed a_o and has started to travel back towards the right wall near $\hat{t}$ = 1.0. Since the overheat ratio is high, the wave travels faster than the reference acoustic speed a_o , particularly near the heated wall. Hence, the wave is found to traverse a longer length (than the cavity width) in time $\hat{t}$ = 1.0. The same applies to the location of the waves at

$\hat{t}$ = 1.5 and $\hat{t}$ = 2.0. For lower overheat ratios (shown later) the wave travels at a speed close to the reference acoustic speed. The dashed line in the figure is the solution at $\hat{t}$ = 0.25 from a one-dimensional analysis by (Huang and Bau, 1997) for a similar (albeit one-dimensional) problem. The agreement between the two solutions is very good. For a coarser grid (300 x 50), the present model predicts the location of the wave front accurately. However, finer grids (400 x 50) were required to match the height of the wave with the solutions given by (Huang and Bau, 1997).

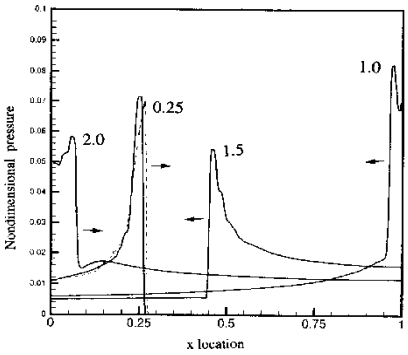

Fig.2 Normalized pressure as a function of the normalized horizontal distance

Figure 3 depicts the pressure variation as a function of time at the mid-point of the right wall for the case shown in Figure 2. The pressure at the right wall remains unchanged until the thermoacoustic wave reaches it. The pressure then rises almost instantaneously, and then decreases gradually. The pressure increases sharply again when the wave finally travels back to the right wall after traveling the width of the cavity twice. The peak broadens with time, and nonlinear effects eventually distort the pressure peaks. Eventually, these oscillations are damped and the pressure reaches a new equilibrium value, due to the energy input to the system via the left wall.

Strength of the pressure wave is strongly correlated to the overheat ratio and pressure oscillations are damped with increasing time.

Long time solutions

Results are shown in Fig. 4 for the midpoint pressure of the enclosure, where the Rayleigh number is 10^4.

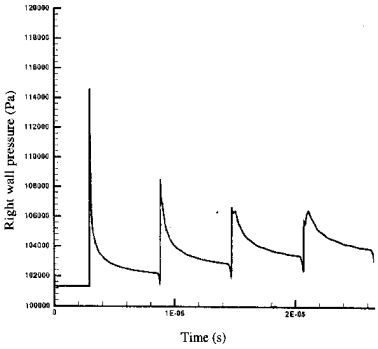

Fig. 3 Pressure variation in the midpoint of the right wall as a function of time

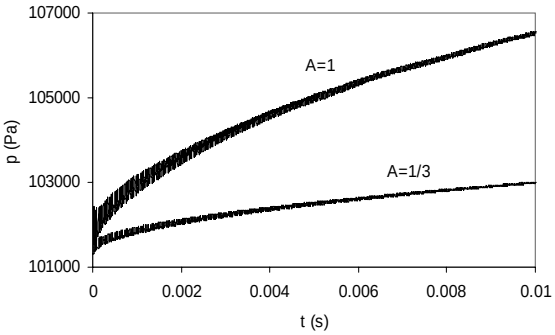

Fig. 4 Variation of pressure with time at the midpoint of the enclosure for two different overheat ratio

In practice, due to the thermal inertia of the wall and a heating system and unavoidable heat losses to the environment, it is difficult to generate a step change (impulsive heating) in the wall temperature. Therefore, the effect of the rapidity of the wall heating process (gradual heating) on the thermoacoustic wave behavior was investigated and results are shown in Fig.5 (A=1/3 and Ra=10^4) for the time variation of the midpoint pressure for three different heating conditions.

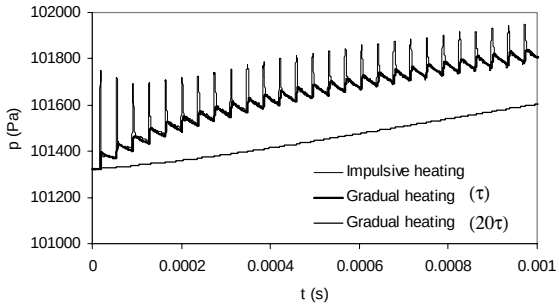

Fig. 5 Effect of the rapidity of the left wall heating process on the midpoint pressure of the enclosure ($\tau = 36.82\times10^{-6}$ s, A = 1/3)

The gradual heating process was considered with an exponential expression:

$$T_L(t) = T_0[1 + A(1 - e^{-t/\tau_h})] \qquad (10)$$

Where τ_h is the time constant of the wall heating process. For impulsive heating, $\tau_h = 0$. For two gradual heating cases given in Fig. 5, τ_h was τ and 20τ, respectively where, τ is the travel time of sound waves for the length of the enclosure. For first gradual heating case ($\tau_h = \tau$) the value for the time constant was identified, below which the physical behavior differs negligibly from that for a step change in the wall temperature. Fig.3 indicates that the rapidity of the wall heating process has very significant effect on the strength of the pressure waves. When $\tau_h = 20\tau$, the strength of the thermoacoustic waves are negligible.

Computations were carried out for longer times at which the buoyancy-induced flow fields develop. In Fig. 6 and 7, results obtained for the x- and y-components of the velocity vector are shown along the horizontal mid-plane of the enclosure for A = 1/3 and Ra = 10^4 at t=0.025 s.

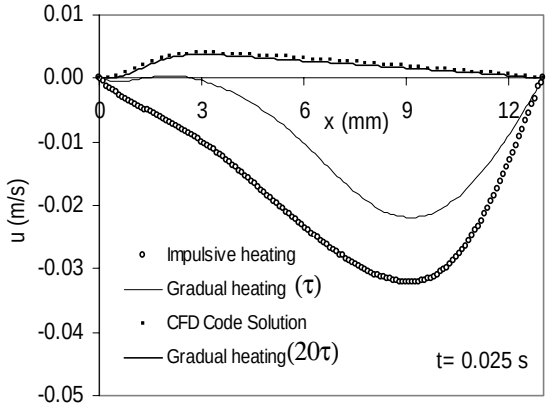

Fig. 6 Variation of the x- component of the velocity vector along the horizontal mid-plane of the enclosure.

These results include FCT solution for the impulsive and gradual heating cases and a pressure-velocity formulation based Navier-Stokes code solution (using the implicit scheme).

For the latter solution, the heating process is rather slow, such that no thermoacoustic waves are generated. These velocity profiles show the significance of the thermoacoustic motion on transient heat convection process. In case of impulsive heating, strong pressure waves completely change the flow characteristics in the enclosure and thermoacoustic wave effect dominates the fluid motion. This effect is very clearly seen by the negative values of the u velocity in Fig. 6. The effect of thermoacoustic waves on v velocity is found less significant (Fig. 7). With gradual heating ($\tau_h=\tau$) thermoacoustic effect losses its power and expected flow characteristics of the buoyancy driven fluid motion is observed (gradual heating, $\tau_h=20\tau$). Fig. 8 (a) –(d) show this process more clearly with the velocity vectors for the case where A=1/3 and Ra=10^4. All four figures show the velocity field in the enclosure at a given time (t=0.025 s), with different heating conditions of the left wall. For impulsive heating, Fig. 8(a), very strong back flow is observed as a result of the pressure wave reflection on the right wall.

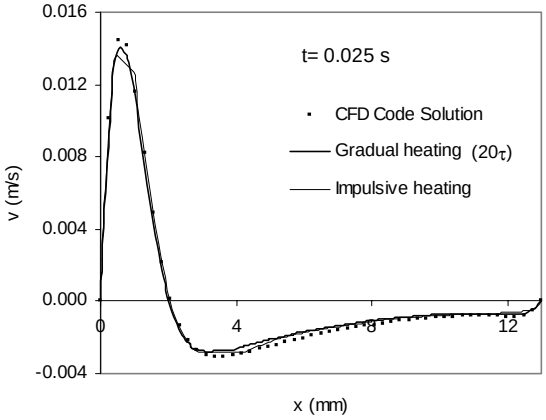

Fig. 7 Variation of the y- component of the velocity vector along the horizontal mid-plane of the enclosure

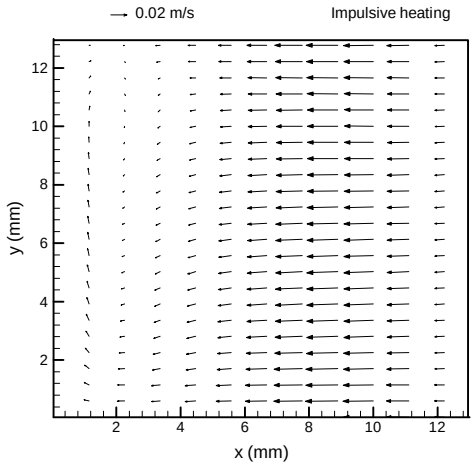

a) Impulsive heating

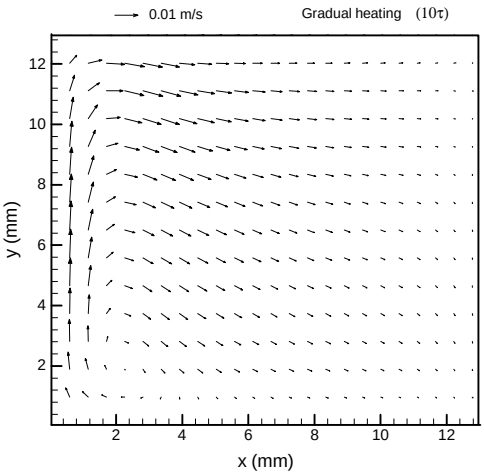

c) Gradual heating (10τ)

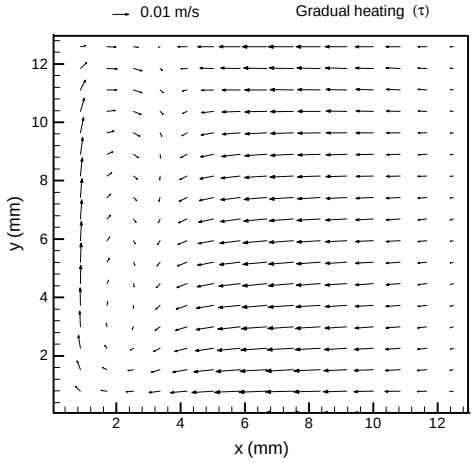

b) Gradual heating (τ)

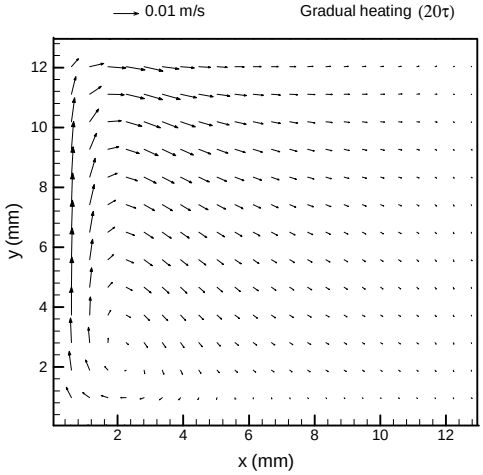

d) Gradual heating (20τ)

Fig. 8 Variation of the velocity vectors and flow field depending on the rapidity of the wall heating process at t = 0.025 s. a) Impulsive heating, b) Gradual heating (τ), c) Gradual heating (10τ), d) Gradual heating (20τ)

This behavior significantly changes in case of gradual heating as shown in Fig. 8(b), 8(c), and 8(d). The effect of pressure waves on the process decay with increasing time. It is interesting to note that though the characteristic time for acoustic wave propagation in the enclosure ($\tau = 36.82\times10^{-6}$ s) is rather small, the effects of the thermoacoustic waves are significant even at t = 0.025 s, as shown in Fig. 8.

Traditional computational fluid dynamics techniques employing pressure-velocity formulation of the Navier-Stokes equations fail to predict the thermoacoustic effect on the transient buoyancy driven motion. In earlier studies (Ozoe et al., 1980; Ozoe et al., 1990), the signature of the thermoacoustic waves were not predicted accurately – perhaps due to significant numerical diffusion and the lack of 'characteristic' type wall boundary conditions in the scheme (Poinsot and Lele, 1992). The flow fields given in the earlier papers also do not clearly demonstrate the effects of thermoacoustic waves on the buoyancy-induced flows. Corresponding pressure fields for impulsive Fig. 8(a) and gradual heating ($\tau_h=10\tau$, Fig. 6(c)) cases are given in Fig. 9(a) and Fig. 9(b), respectively. In case of impulsive heating Fig. 9(a), pressure in the enclosure is relatively high and is not changing on the vertical direction.

Effect of fluid properties

The effect of fluid properties on the thermoacoustic phenomena was also investigated by considering helium filled enclosure. Helium has approximately nine times larger thermal diffusivity than nitrogen. With the same overheat ratio (A=1/3) and same temperature difference (T_L-T_R) for nitrogen and helium cases, thermoacoustic waves generated by sudden (impulsive) heating of the left wall of the enclosure travel faster and generate stronger pressure waves in helium Fig. 10(a). Very high heat transfer coefficients are achieved at the right wall of the enclosure at the instances when the acoustic waves impinge on the wall Fig. 10(b). For same heating condition, computations were carried out for longer time to see the development of the flow field.

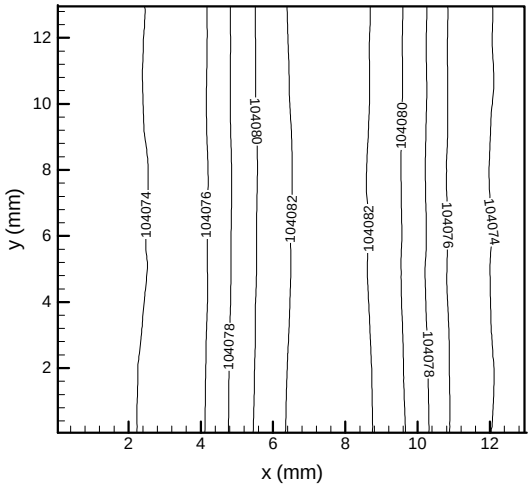

a) Impulsive heating

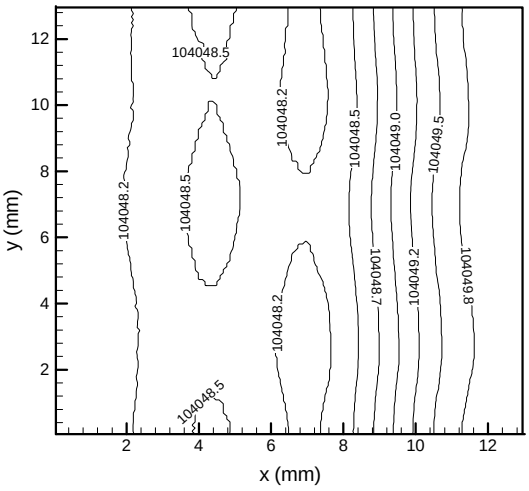

b) Gradual heating (10τ)

Fig. 9 Variation of pressure in the enclosure at t = 0.025 s: a) Impulsive heating, b) Gradual heating (10τ)

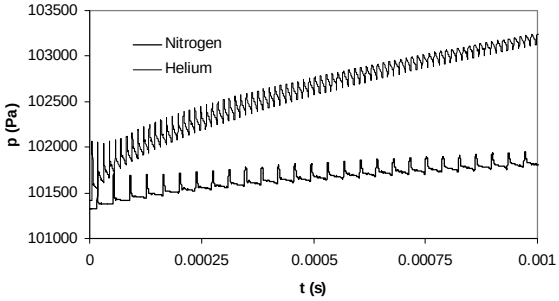

a) midpoint pressure

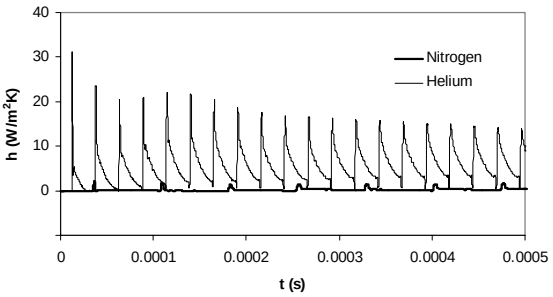

b) Right wall heat transfer coefficient

Fig. 10. Effect of thermoacoustic wave motion on a) midpoint pressure and b) right wall heat transfer coefficient of the enclosure for two different gases

Results are shown in Fig. 11(a) and 11(b) for nitrogen and helium at t = 0.01 s, respectively. For both cases temperature difference (T_L-T_R) and geometry are same. In nitrogen Fig. 11(a), thermoacoustic waves and resulting flow are relatively strong and flow filed is one-dimensional. However, in helium buoyancy-driven flow development is starting earlier, as shown in Fig. 11(b).

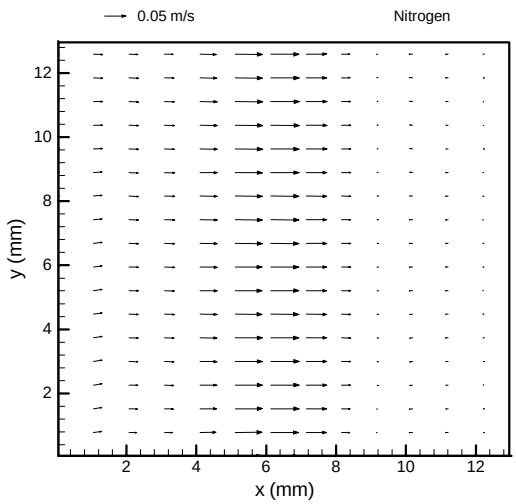

a) Nitrogen

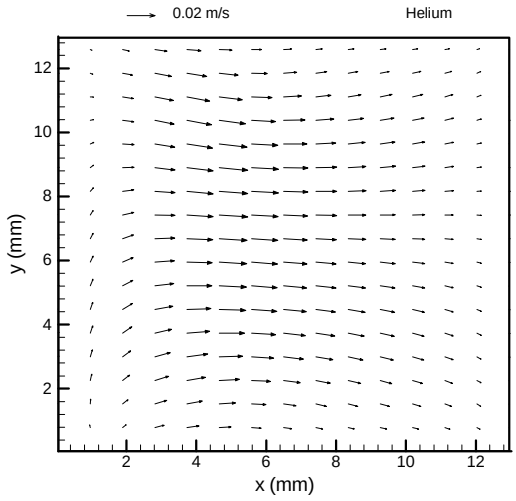

b) Helium

Fig. 11. Distribution of the velocity vectors in the flow field for two different gases at t = 0.01 s. a) Nitrogen, b) Helium

The effect of the gravitational acceleration was found negligible at the early stages of the flow development and thermoacoustic behavior.

Thermoacoustic streaming

It is well known that interaction between a solid object and fluid in an oscillating flow field creates secondary flows called acoustic streaming (Zarembo, 1971). We simulated the flow field within the enclosure caused by a sinusoidally varying left wall temperature where

$$T_L(t) = T_0 + T_0 * A * \sin(\omega t) \qquad (11)$$

with

T_0=300 K
A = 1/3

and f = $\omega/2\pi$ = 20 kHz

The right wall is maintained at 300 K and the top and the bottom walls are insulated as before. As the wall temperature fluctuates, a corresponding pressure wave travels down the enclosure. Time-dependent calculations were carried out for 500 cycles. Fig. 12 shows the instantaneous distribution of the velocity vectors in the enclosure at the end of the 500 cycle.

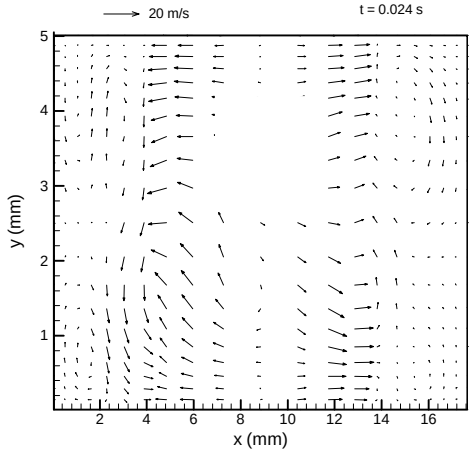

Fig. 12 Instantaneous velocity field at the end of 500 cycles

This primary flow field changes with time as the left wall temperature undergoes variation. The time-averaged results for the last 100 cycles of the computations (Fig. 13) show a non-zero velocity field, indicating the existence of steady 'thermoacoustic streaming'. Fig. 14 shows the corresponding streamlines for the case given in Fig. 13. For streaming motion to occur, velocity field must be a combination of two components, a primary un-steady component and a secondary steady component.

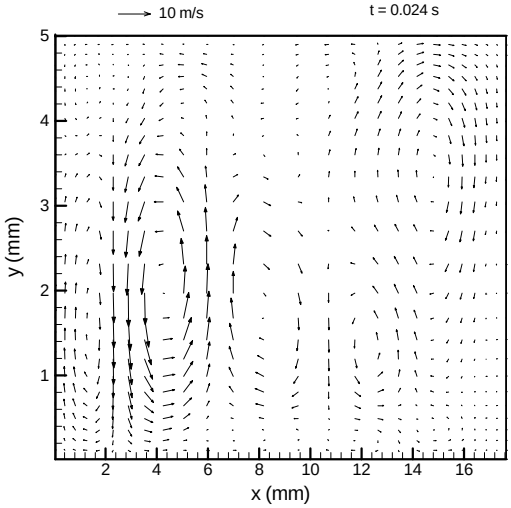

Fig. 13 Time averaged velocity field (between 400 – 500 cycles)

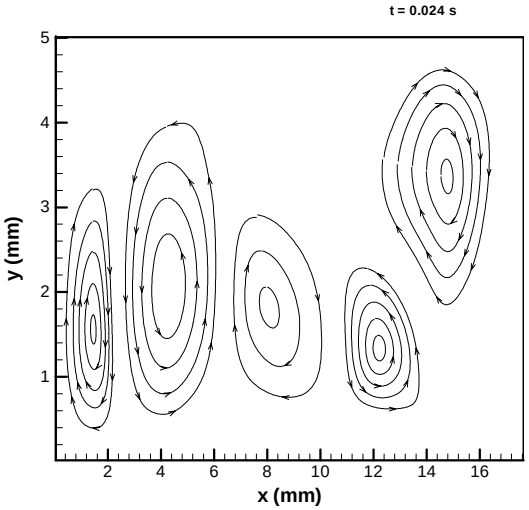

Fig. 14. Time averaged flow filed in the enclosure (corresponding streamlines)

CONCLUSIONS

The effects of the thermoacoustic waves on the transient natural convection process in an enclosure were studied by solving the unsteady compressible Navier-Stokes equations. The significant effects of the pressure waves on the transient natural convection process and flow development are determined by utilizing highly accurate FCT algorithm. Significant effect of the fluid thermal diffusivity on the thermoacoustic convection was observed. It was also shown for the first time that a rapidly fluctuating wall temperature can cause steady streaming flows in the enclosure.

REFERENCES

J. P. Boris, A. M. Landsberg, E. S. Oran, and J. H. Gardner, LCPFCT- A flux-corrected transport algorithm for solving generalized continuity equations, Naval Research Laboratory NRL/MR/6410-93-7192, Washington, DC, April 16, 1993.

M. A. Brown and S. W. Churchill, Experimental measurements of pressure waves generated by impulsive heating of a surface, AIChE Journal, vol. 41, pp. 205-213, 1995.

M. A. Brown and S. W. Churchill, Finite-difference computation of the wave motion generated in a gas by a rapid increase in the bounding temperature, Computers and Chemical Engineering, vol. 23, pp. 357-376, 1999.

S. W. Churchill and M. A. Brown, Thermoacoustic convection and the hyperbolic equation of conduction, International Communications in Heat and Mass Transfer, vol. 14, pp. 647-655, 1987.

B. Farouk, E. S. Oran, and T. Fusegi, Numerical study of thermoacoustic waves in an enclosure, Physics of Fluids, vol. 12, pp. 1-10, 2000.

B. Farouk, E. S. Oran, and K. Kailasanath, Numerical Simulation of the Structure of Supersonic Shear Layers, Phys. Fluids A, vol. 3, pp. 2786-2798, 1991.

Y. Huang and H. H. Bau, Thermoacoustic waves in a semi-infinite medium, International Journal of Heat and Mass Transfer, vol. 38, pp. 1329-1345, 1995.

Y. Huang and H. H. Bau, Thermoacoustic waves in a confined medium, International Journal of Heat and Mass Transfer, vol. 40, pp. 407-419, 1997.

H. Ozoe, N. Sato, and S. W. Churchill, The effect of various parameters on thermoacoustic convection, Chemical Engineering Communications, vol. 5, pp. 203-221, 1980.

H. Ozoe, N. Sato, and S. W. Churchill, Numerical analyses of two and three dimensional thermoacoustic convection generated by a transient step in the temperature of one wall, Numerical Heat Transfer, Part A, vol. 18, pp. 1-15, 1990.

M. Parang and A. Salah-Eddine, Thermoacoustic convection heat-transfer phenomenon, AIAA Journal, vol. 22, pp. 1020-1022, 1984.

T. J. Poinsot and S. K. Lele, Boundary conditions for direct simulations of compressible viscous flows, Journal of Computational Physics, vol. 101, pp. 104-129, 1992.

L. Trilling, On thermally induced sound fields, The Journal of the Acoustical Society of America, vol. 27, pp. 425-431, 1955.

B. Zappoli, S. Amiroudine, P. Carles, and J. Ouazzani, Thermoacoustic and buoyancy-driven transport in a square side-heated cavity filled with a near-critical fluid, Journal of Fluid Mechanics, vol. 316, pp. 53-72, 1996.

L. K. Zarembo: Acoustic Streaming. *In* L. D. Rozenberg (ed.): *High Intensity Ultrasonic Fields*, pp. 137-199, Plenum Press, 1971